

Snow Cover Patterns and Evolution at Basin Scale: GEOTop Model Simulations and Remote Sensing Observations

STEFANO ENDRIZZI,¹ GIACOMO BERTOLDI,² MARKUS NETELER³ AND RICCARDO RIGON¹

ABSTRACT: Remote sensing data can provide images of snow covered areas and, therefore, it is possible to follow the time evolution of snow melting spatial patterns with increasing spatial and temporal resolution. Snow cover patterns are dominated by the complex interplay of topography, radiation forcings and atmospheric turbulent transfer processes. The snow cover evolution in an alpine basin in Trentino (Italy) is here studied, comparing the simulations of the distributed hydrological model GEOTop with remotely sensed data. GEOTop describes the soil-snow-atmosphere energy and mass exchanges, taking into account the snow physics and the topographic effects of elevation, slope and aspect on solar radiation and air temperature. The Snow cover extent has been provided by MODIS 8-day composite maps with a resolution of 500 metres. The model reproduces the physical features of snow melting reasonably and shows a fair agreement with the data. The relative importance of precipitation, solar radiation, and temperature to control the snow accumulation and melting processes is also investigated.

Keywords: snow water equivalent, distributed modelling, remote sensing, topography

INTRODUCTION

To have information about the evolution of the snow cover extent and the snow water equivalent is very useful for the water resource management, and in relation to climate change. So far temperature index models, like SRM (Martinec and Rango, 1986), based on a statistical relation between snow melting and temperature, have been widely used. Although many of these models have evolved so that topographic effects could be considered (Cazorzi and Dalla Fontana, 1995), distributed physically based models, like ISNOBAL (Marks et al., 1999) can provide more detailed information about snow physics and improved predictions of snow cover. Their application also allows to study what phenomena may be important in snow accumulation and melting, and what may be the sensitivity to changes of atmospheric forcing.

At the same time, remote sensing data are available with improved spatial and temporal resolution (for example MODIS (Hall et al., 2002) and NOHRSC (Hall et al., 2000)). Several models, using remote sensing data as input (Turpin et al., 1999) or to perform data assimilation (Carroll et al., 2006), have been recently developed. However, in mountain basins, remote sensing data can be affected by some errors, and consistent physical modelling maintains great

¹ Department of Civil and Environmental Engineering, University of Trento, Via Mesiano 77, 38050 Povo (TN), Italy, email: stefano.endrizzi@ing.unitn.it

² Department of Civil and Environmental Engineering, Duke University, Durham, NC, USA

³ ITC-IRST, Center for Scientific and Technological Research, 38050 Povo (TN), Italy

importance, because snow cover patterns are dominated by the complex interplay of topography, radiation forcing and atmospheric turbulent transfer processes (Pomeroy et al., 2003).

The GEOTop model (Rigon et al., 2006) is a distributed hydrological model that solves the energy and water balance on a landscape whose topographical surface is described by a digital elevation model. The model has been conceived to be applied to mountain basins characterized by complex topography, where snow accumulation and melting have to be accounted. GEOTop includes a snow module, the first version (version 0.875) of which was the object of a previous work (Zanotti et al., 2004), where its capability to predict the snow water equivalent (SWE) evolution in a point was tested, and the results were compared with local measurements. In Zanotti et al. (2004) an application on a small mountain basin with a surface area of a few square kilometres was then presented, but the results could not be checked in more than one measurement point. Since then, the snow cover module in GEOTop has been improved (version 0.9375) such that a multilayer representation has been implemented, similar to the one of the CLM land surface model (Oleson et al., 2004). The GEOTop snow module is quite similar to ISNOBAL (Marks et al., 1999), as it solves the snow energy balance, but it is part of a complete hydrological model that considers the whole soil-snow system. The next step is to predict the snow cover evolution and its variability at the distributed scale.

Some works have been published about the temporal distribution of snow cover, for example Alfnes et al. (2004) using statistical tools. In order to do this, a distributed field of the meteorological forcing as input data is needed, or, if only a few measurement stations are available throughout the basin, we need to find some criteria to spatially extrapolate the measurements, although they might lead to some errors.

An application in an Alpine basin with surface area of about 250 square kilometres is shown here. The snow cover extension area is compared with corresponding maps provided by remote sensing techniques. In particular, MODIS maps (Hall et al., 2002; Riggs et al., 2003) have been used because the Aqua and Terra satellites overpass locations daily. Snow products are delivered at a spatial resolution of 500 metres, which is sufficient to keep the signature of the topographic features in an Alpine environment (Cline et al., 1998) where the snow cover spatial distribution is strongly dependent on aspect and elevation. In addition, the MODIS data are easily available for applicative uses.

Snow cover maps provided by remote sensing have already been used, mainly as an auxiliary to the models (Lee et al., 2005; Turpin et al., 1999), but here they are used only to check the model results. The problem of the initial SWE distribution does not exist as the simulation starts from a late summer initial condition, when in the considered basin no snow is present.

Our aim in this paper is to test the capability of the model to reproduce a realistic snow cover evolution during a whole winter season and to investigate the relative importance of precipitation, solar radiation, and temperature to control the snow accumulation and melting processes in an Alpine environment, with reference to its time evolution and its dependence on elevation and aspect. We want to develop a modelling framework as physically based as possible, though parsimonious in its input data requirements and, therefore, easily applicable for operational use (Carroll et al, 2006).

THE MODEL

The GEOTop model has been fully described in Rigon et al. (2006) and in Bertoldi et al. (2006). This model has been conceived to be an integration of a rainfall-runoff model and a land surface model as it solves the three-dimensional soil water budget equation together with the one-dimensional energy budget equation, so that it can calculate the spatial distribution of many hydro-meteorological variables (such as soil moisture, surface temperature, convective and radiative fluxes) without losing the main purpose of hydrological models, that is predicting the water discharge at a specific closure section. However, this paper is focused on the simulation of the spatial patterns and of the time evolution of the snow covered area and of the SWE at basin scale.

In the following paragraph the main improvements of the snow module with reference to the version presented in Rigon et al. (2006) are briefly discussed.

In the version 0.9375 of the snow module in GEOTop, the snow cover is described with a multilayer scheme. For each snow layer the liquid and solid water budget equations and the energy budget equation are solved together with the continuity equation and a formula linking the phase change with the temperature. So five equations for the following five unknowns are available: liquid and ice contents, porosity, snow temperature, and amount of water changing phase.

The water budget equations, for liquid water and ice, are expressed as follows:

$$\theta_w = \frac{1}{\rho_w} \left(\frac{\partial W}{\partial t} + \frac{\partial Q_w}{\partial z} \right) \quad (1)$$

$$\theta_i = \frac{1}{\rho_i} \left(\frac{\partial W}{\partial t} + \frac{\partial Q_i}{\partial z} \right) \quad (2)$$

where θ_w and θ_i are the nondimensional liquid water and ice content, t is time, z the vertical coordinate (positive upwards), ρ_w and ρ_i the density of liquid water and ice, respectively, Q_w and Q_i the vertical flux of liquid water and ice (the latter is equal to 0 except at the snow-atmosphere interface where it becomes the snow precipitation), and W is the amount of water changing phase (positive in the case of melting, negative in the case of freezing). As the liquid water flow inside the snow cover is mainly due to gravity, the equations are solved only in the vertical direction, neglecting the lateral flow inside the snowpack, but not in the underlying soil. Q_i depends on the liquid water fraction in the snow exceeding the capillary retention as in Colbeck and Anderson (1982).

The energy budget equation is the following:

$$C \frac{\partial T}{\partial t} + L_f \frac{\partial W}{\partial t} = \frac{\partial}{\partial z} \left(k \frac{\partial T}{\partial z} \right) + \frac{\partial (Q_w U_w)}{\partial z} \quad (3)$$

where T is the temperature, L_f the latent heat of fusion, U_w the specific energy content of the liquid water, and k and C the thermal conductivity and the thermal capacity, respectively, calculated as averages of the values of the different phases present. The equation (3) is solved with the following boundary condition at the snow-atmosphere interface, where the exchange fluxes occur:

$$\left(k \frac{\partial T}{\partial z} \right) = -R_n + H + L \quad (4)$$

where R_n is the net radiation, H the sensible heat flux and L the latent heat flux (both positive upwards). The treatment of radiation is essentially the same as in Zanotti et al. (2004). The effects of shadowing, slope and aspect, which are extremely important in a complex topography, are taken into account for direct shortwave radiation, and the sky view factor is considered for the diffuse shortwave radiation and for the longwave radiation. Shortwave radiation is parameterized as in Iqbal (1983). Longwave radiation is calculated using Stefan-Boltzmann formula. Whereas the outgoing longwave radiation is clearly dependent on the surface temperature, there are some uncertainties in calculating the incoming longwave radiation, as the latter depends on the entire profile of the air temperature above the snowpack. Different experimental formulae, as those of Brutsaert (1975), Satterlund (1979), and Idso (1981), that parameterize this component of radiation in function of the skin temperature, have been used. The convective heat fluxes are calculated after Monin-Obukhov similarity theory, using the stability function of Businger et al. (1981). As they depend also on surface temperature, which is unknown as long as the energy budget is not solved, some iterations are needed.

The continuity equation correlates the different phases in the snowpack:

$$\theta_w + \theta_i + \theta_v = 1 \quad (5)$$

where θ_v is the nondimensional gas and vapour content, that is the porosity.

Finally, we need to find a relation between the snow temperature and the phase change. We have chosen that the phase change should occur when the temperature in each snow layer is equal to 273.15 K: neither the temperature is allowed to increase as long as ice is present nor can it decrease until liquid water is entirely frozen. Therefore,

$$W \neq 0 \quad \text{if} \quad T = 273.15K \quad ; \quad W = 0 \quad \text{if} \quad T \neq 273.15K \quad (6)$$

Thus the system of equations (1)-(2)-(3)-(5)-(6) is solved with a finite difference method with respect to the unknowns T , W , θ_w , θ_i , θ_v .

The snow layers have a varying thickness in accordance with the snow precipitation and snow metamorphism (Anderson, 1976). The algorithms to combine and subdivide snow layers have been taken from Oleson et al. (2004), which makes it possible to describe the density changes of the snow pack.

APPLICATION

The model has been applied to the upper part of Brenta Basin (Trentino, Italy), in the Eastern Italian Alps, a basin with a surface area of about 250 square kilometres. Its elevation ranges from 340 m a.s.l. to 2303 m a.s.l., and the land cover is very variable. The bottom of the valley is urbanized, and many small villages are present, although there is still a wide countryside area. Two lakes, with total area of about 6 square kilometres, are also present. They play an important role in the regulation of the discharge, but, as here our main interest is to follow the snow cover evolution, they are neglected. As elevation increases, woodland prevails, even if there are some small resort villages and wide grassland and pasture areas. The vegetation limit ranges from 1900 m a.s.l. to 2000 m a.s.l.. The snow cover has been simulated for the season 2003-2004, namely from 16th October 2003 to 16th June 2004, using a model grid resolution of 250 m.

METEOROLOGICAL DATA

For the time considered, hourly precipitation measurement data were available for 15 stations located in the basin or in the nearby areas. Precipitation was then distributed according to kriging techniques, and it was split into liquid and solid form in conformity with the air temperature, defining a threshold air temperature T_L above which the precipitation is always liquid and another threshold temperature T_S below which the precipitation is always solid, as in U.S. Army Corps of Engineers (1956). These threshold temperatures are considered tuneable and adjustable parameters. In fact, as discussed later, in order to catch the snow events with precision, it results very important to distribute the air temperature in the basin accurately.

Hourly air temperature observations performed in 17 meteorological stations in and around the basin were used to find a linear dependence of the temperature on the elevation, which is considered variable in time, but valid all over the basin, and an hourly value of the lapse rate was found.

Figure 1 shows the relation between the air temperature measurements averaged on the whole season and the station elevations. The temperature variation presents a clear linear trend with a lapse rate of 3.9 °C/km (regression constant equal to 0.94), which is lower than the lapse rate normally used (6.5 °C/km). This means that at the annual scale the temperature measurements do not exhibit evident and regular variability with the horizontal coordinates. However, some stations located approximately at the same elevation can record temperature differences of some degrees (at the most 2 °C) due to local factors (for example shadowing) and to particular meteorological events. This could be a measure of the error in the temperature estimation.

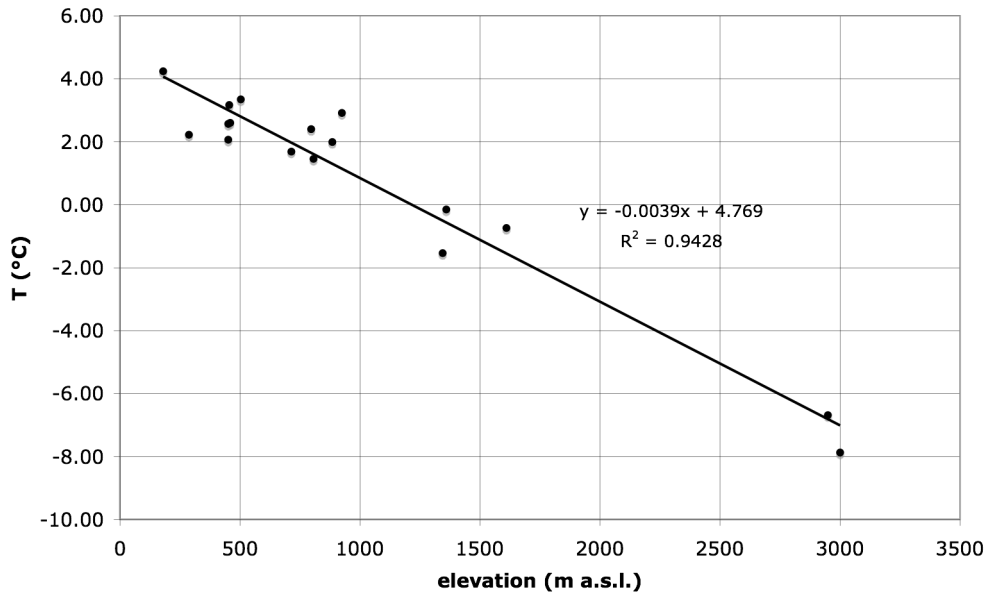


Figure 1: Variation of the season average of the air temperature measurements with the elevations of the meteorological stations (dots), and regression line.

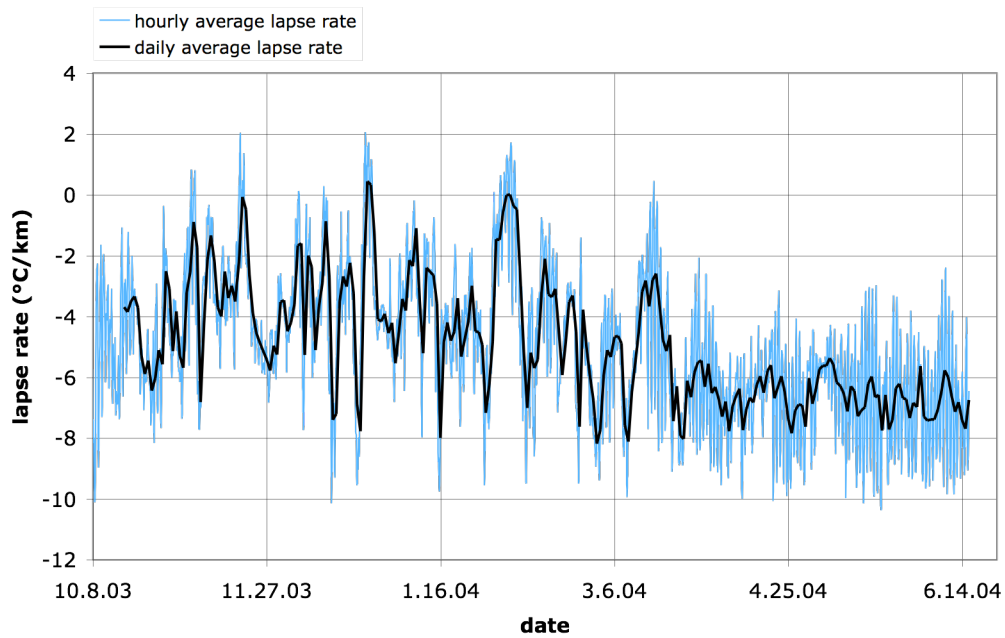


Figure 2: Time evolution of the hourly and daily average lapse rate inferred by the measurements.

But if the time evolution of the lapse rate, daily and hourly averaged (Figure 2) is plotted, it can be noticed that during the winter there are frequent periods of thermal inversion, with a nearly isotherm atmosphere, but during the spring time the lapse rate is more clearly defined and reaches values around the adiabatic lapse rate. The lapse rate also shows a typical daily cycle, with a marked nocturnal inversion in winter. The definition of a correct value of the lapse rate is critical to capture the correct snow-rain limit. Therefore, we have chosen to use an hourly varying lapse rate as input data for the model.

The relative humidity and the wind velocity are kept constant all over the basin.

PARAMETERS OF THE MODEL

The parameters of the model were guessed in order to obtain the best agreement with the remote sensing data. By all means, only a few parameters are important for the snow cover description. They are the temperature roughness length, the wind velocity roughness length, the capillary water amount retained by the snow, and the threshold temperatures aforesaid. The following table reports the value of these parameters with the reference.

Table 1. Main parameters of the snow module in GEOtop

Value	Parameter	Description	Reference
0.05	z_{0T}	Temperature roughness length [m]	Calibration
0.5	z_{0V}	Wind velocity roughness length [m]	Calibration
0.04	S_r	Liquid water in snow retained by capillarity forces, as fraction of porosity [-]	Jordan (1991)
2.0	T_L	Temperature above which all the precipitation is rain [°C]	Calibration
0.5	T_S	Temperature below which all the precipitation is snow [°C]	Calibration

MODIS

The Moderate Resolution Imaging Spectroradiometer (MODIS) is a 36-channel sensor measuring the spectral range from visible to thermal-infrared. It was launched as part of the payload of the Terra (12/1999) and Aqua (5/2002) satellites. Among other products, daily and 8-day composite snow related maps are produced at 500 m and 1000 m resolution. The maps created over land include daily snow albedo and 8-day maximum snow extent. For the latter multiple days of observations for a cell are examined. If snow cover is found for at least one day the cell is indicated as snow. Other values are lake ice, cloud, ocean, inland water and land. If no snow is found in the cell, the most frequent value of the other classes is assigned. Due to the 8-day compositing technique, the impact of clouds is minimized (Riggs et al., 2003).

In this study we have used the MOD10A2 8-day composite maximum snow extent data at level V004. The data were processed in GRASS GIS (Neteler, 2005).

However, MODIS snow cover maps can be affected by some errors, the most common of which are the errors of commission. This means mapping cells as snow covered when the occurrence of snow is extremely unlikely. These errors are usually associated with the least favorable conditions of illumination and cloud type for optimal snow mapping (Riggs and Hall, 2006).

COMPARISON BETWEEN THE RESULTS OF THE MODEL AND MODIS DATA

Snow covered area spatial distribution

In this paragraph the MODIS 8-day maximum snow extent maps and the corresponding 8-day GEOtop model output maps are compared. The snow free area is reported in green, and the snow covered area is in white. Whereas MODIS can only provide information about the presence of snow, the model gives results about the amount of SWE, which is reported in the pictures in white-blue colour scale. Five pairs of maps have been chosen as representative of the main qualities and problems of the models.

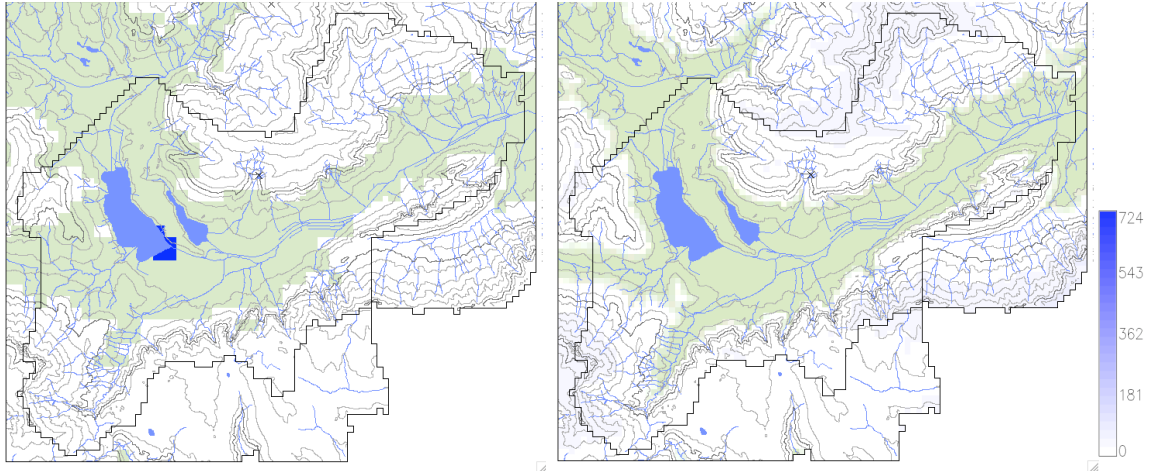


Figure 3: 8-day composite maps (24th October 2003) for snow cover obtained by MODIS (left) and by the model (right). The snow free area is reported in green, the snow covered area is in white in MODIS map, in white-blue colour scale (legend on the right) in the model map.

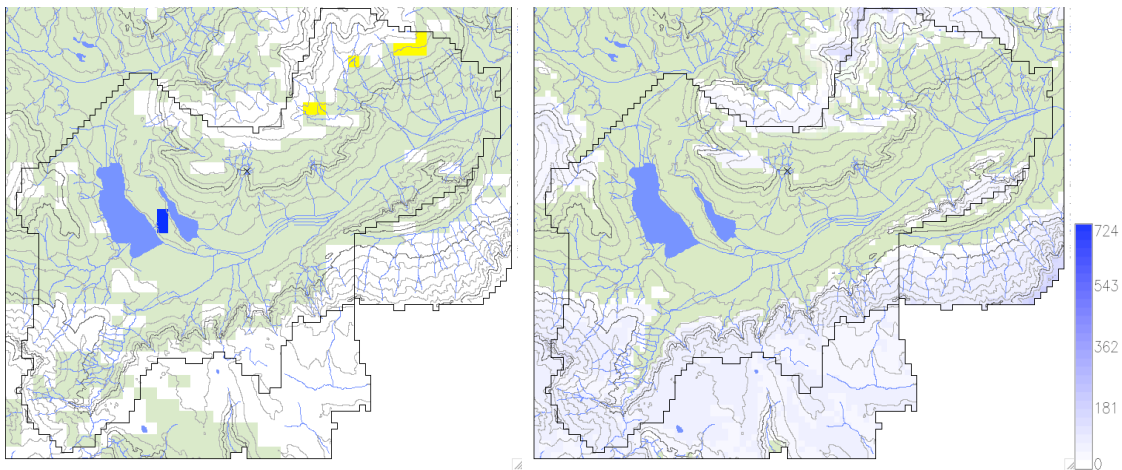


Figure 4: 8-day composite maps (17th November 2003) for snow cover obtained by MODIS (left) and by the model (right). The snow free area is reported in green, the snow covered area is in white in MODIS map, in white-blue colour scale (legend on the right) in the model map.

The first pair of pictures (Figure 3) regards the autumn season: snow cover is present only at the highest elevations, and the model predicts reasonably the snow limit. However, in the model output map the snow limit strictly follows the elevation contour lines, because snow precipitation mainly depends on the air temperature, which, in turn, depends only on elevation. In the MODIS map the snow limit is close to the elevation contour, but there are some deviations probably due to local variations of air temperature, or, simply, to the coarser resolution of the MODIS maps (500 m grid cell) than in the model maps (250 m grid cell).

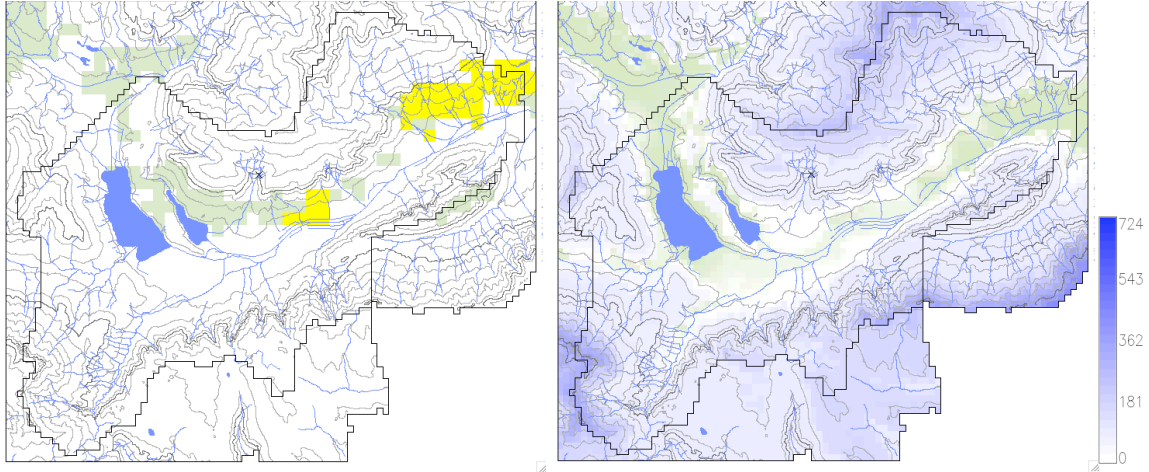


Figure 5: 8-day composite maps (17th January 2004) for snow cover obtained by MODIS (left) and by the model (right). The snow free area is reported in green, the snow covered area is in white in MODIS map, in white-blue colour scale (legend on the right) in the model map. The pixels for which it was not possible to detect snow due to cloud cover are in yellow.

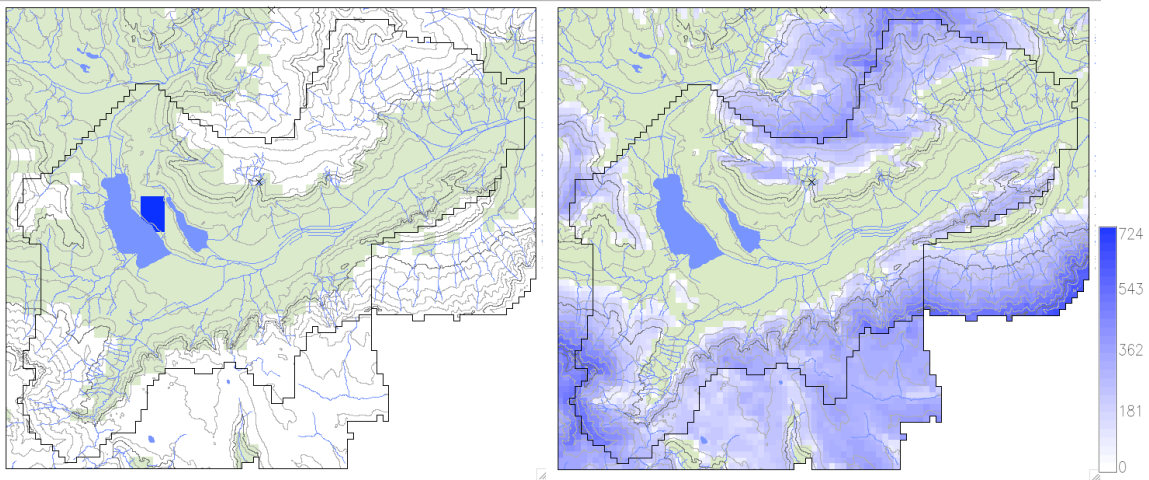


Figure 6: 8-day composite maps (29th March 2004) for snow cover obtained by MODIS (left) and by the model (right). The snow free area is reported in green, the snow covered area is in white in MODIS map, in white-blue colour scale (legend on the right) in the model map.

The second pair (Figure 4) is an example of the late autumn season, after several days without solid precipitation. The snow patterns are controlled here also by slope and aspect, and there are some white spots inside the snow free area in the pixels receiving a less amount of radiation. The agreement is fairly good, although not all the white spots agree in detail, but it has to be taken into account that MODIS maps may be affected by some commission errors (for example the white spot located near the lake in the bottom of the valley is very unlikely).

The third pair (Figure 5) represents the snow cover after a snowfall in winter. It is difficult for the model to reproduce the snow in the bottom of the valley, as the air temperature field can be uneven and snow precipitation occurs usually at low elevations when the air temperature is close or even slightly above 0 °C. For this reason the threshold temperature above which the precipitation is always liquid and the threshold temperature below which the precipitation is always solid have been fixed to 2 °C and 0.5 °C, respectively, after some calibrations. These values are a little different from the values proposed in US Army Corps of Engineers (1956), respectively 3 °C and -1 °C. The areas located at the bottom valley are quite large, but they are usually covered by a small amount of snow, which melts quickly.

The fourth pair (Figure 6) is relative to early springtime. The snow patterns are dominated by elevation, as a consequence of late snowfall events, as well as by slope and aspect, as it is possible to appreciate the differential melting in north facing and south spacing slopes, even though in the two maps the snow limit can be slightly different. In this time SWE reaches its maximum value at the highest elevations.

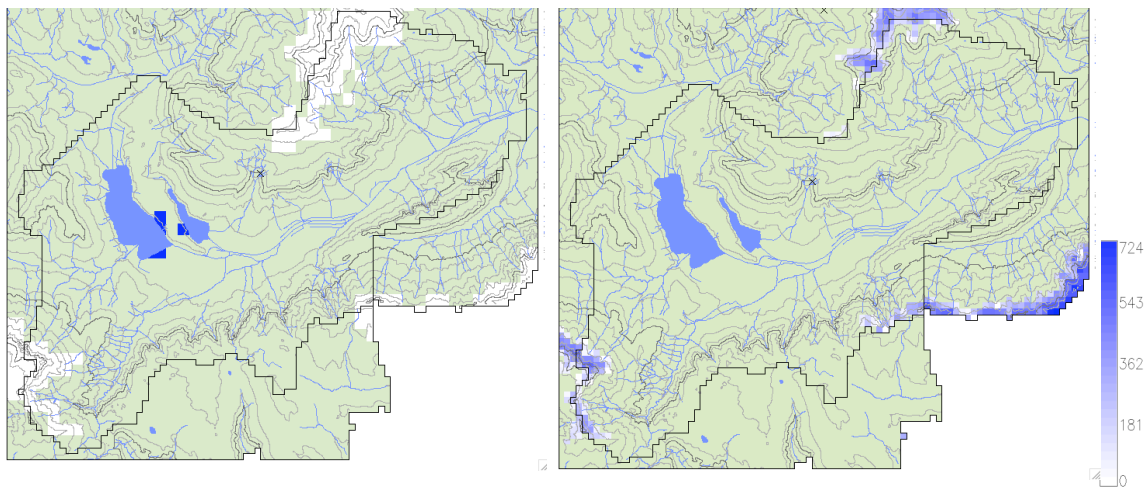


Figure 7: 8-day composite maps (16^h May 2004) for snow cover obtained by MODIS (left) and by the model (right). The snow free area is reported in green, the snow covered area is in white in MODIS map, in white-blue colour scale (legend on the right) in the model map.

Finally, the fifth pair (Figure 7) refers to late springtime: snow cover is present only at the highest elevations, and the snow patterns in the two maps are similar. However, the model result map shows a little faster melting on the south facing slopes than the MODIS map, which, on the other hand, may also be affected by commission errors, because it shows a snow limit lower in the south facing slopes than in the north facing slopes.

In conclusion, the model seems to catch quite well the main patterns of the snow cover extent, which are dominated firstly by elevation, and secondly by slope and aspect. In order to reproduce the snow cover in the best way, it seems crucial to catch the snowfall elevation limits, and to calculate accurately the radiation fluxes and the radiation topographic controls, which play a fundamental role in melting.

Snow covered area as a fraction of total area

The model simulates SWE as a continuous variable and, therefore, a SWE threshold value should be chosen to consider the pixel as entirely covered by snow. Figure 8 reports the evolution in time of the snow covered surface as fraction of the total basin area, using threshold values of 1

mm or 10 mm. This has been done to draw a better comparison between the model and the remote sensing data, as MODIS cannot detect snow if SWE is very small. Moreover, the MODIS data are sometimes affected by uncertainty due to the persistence of cloud cover, and the related range of variability in the snow cover area is shown in the figure.

The agreement is good, in particular in the melting season. However, the limitations of the MODIS 8 day product have to be considered. Large uncertainties during the precipitation periods due to the cloud cover can occur, and the product has a resolution which does not always allow to appreciate the detailed elevation patterns of snow cover, as the mountain basin considered is characterized by strong elevation gradients.

The model underestimates the snow cover extent in the early snow events, probably because it does not predict well the snowfall in the bottom of the valley, which covers quite a wide area. As it has been said in the previous paragraph, it is difficult to distinguish the rain and snow events, because they are not only dominated by the air temperature at the ground, but by the entire temperature profile. The MODIS curve agrees more with the 1 mm threshold model result curve: this probably means that a thin layer of fresh snow in the bottom of the valley, where vegetation is not dense, is easily recognized by remote sensing techniques.

The model snow cover extent is much less sensitive to the threshold value during the spring, when the averaged SWE distribution is higher and more strongly dependent on elevation, as discussed later.

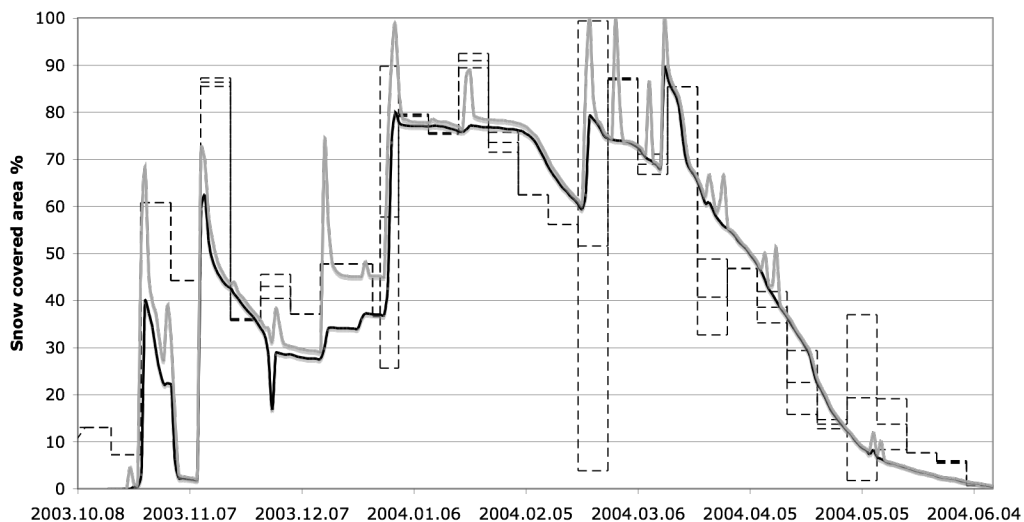


Figure 8: Fraction of the total basin area covered by at least 1 mm (grey continuous line) and 10 mm (black continuous line) of SWE, according to the model results, and snow covered area according to MODIS (dashed black lines) with uncertainty range due to cloudiness against time.

DEPENDENCE OF SNOW COVER ON ELEVATION AND ASPECT

In this paragraph the model results are used to find some relations between SWE, elevation and aspect for the basin considered. The basin is here divided into 10 elevation ranks, each spanning 200 metres. SWE is then averaged in each rank. Figure 9 shows the time evolution of SWE for 4 different elevation ranks, and it can be noticed that its maximum value shifts later into spring as elevation gets higher. At the bottom of the valley a strong snowfall occurred at the beginning of March, but at higher elevations other strong snowfalls occurred later.

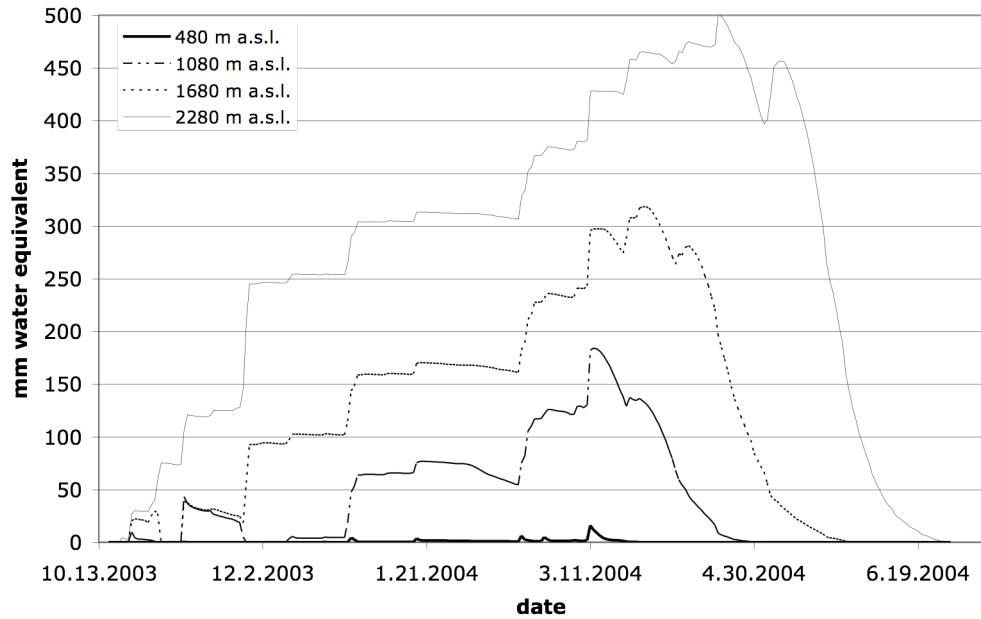


Figure 9: Time evolution of SWE averaged in 4 elevation ranks

The slope of the SWE profile with respect to elevation changes after every snowfall and with the season. Here some examples after 3 different snowfall events - in autumn, in winter, and in early springtime - are shown in Figures 10, 11, and 12.

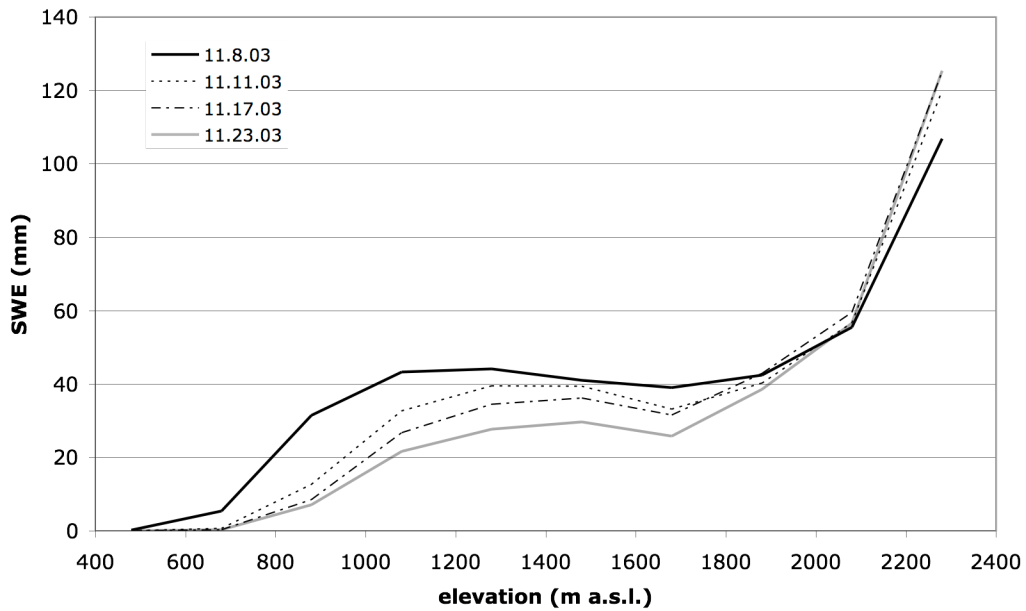


Figure 10: Daily averaged SWE-elevation chart for 4 days after a strong autumn snowfall (occurred on 8th November 2003)

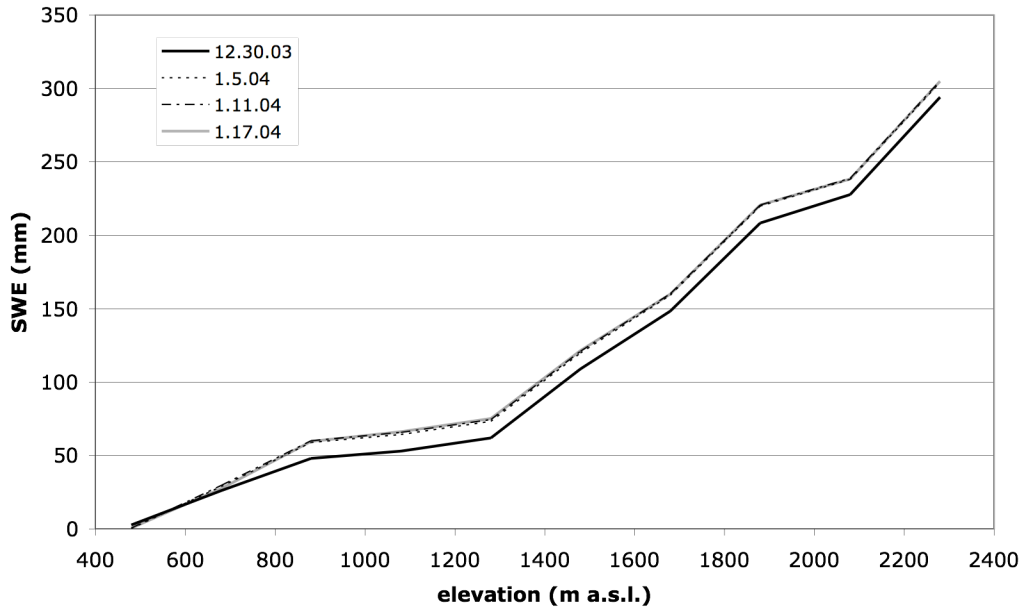


Figure 11: Daily averaged SWE-elevation chart for 4 days after a strong winter snowfall (occurred on 30th December 2003)

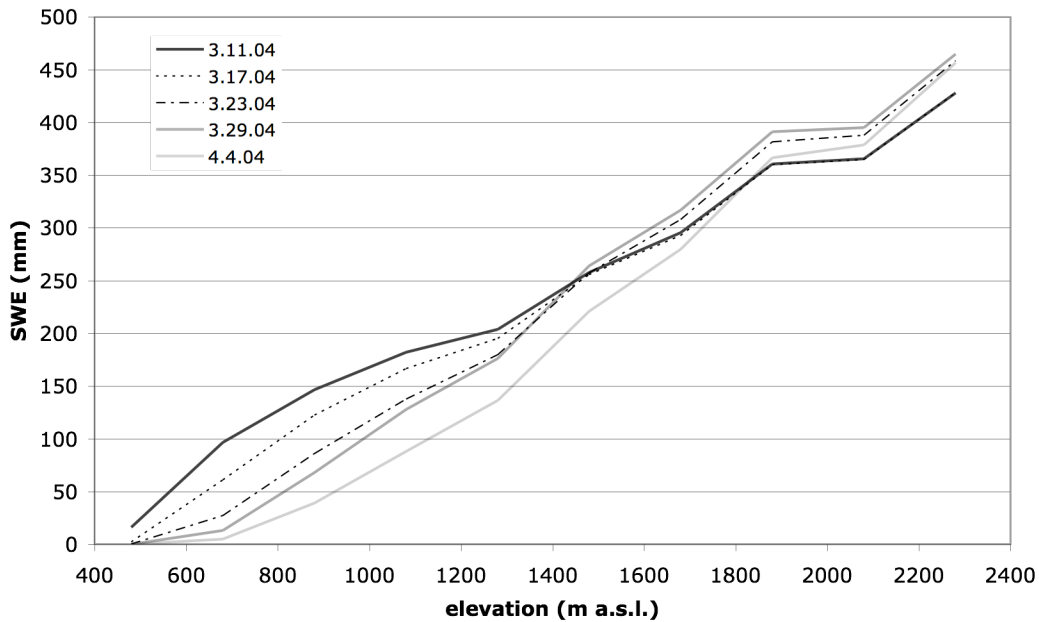


Figure 12: Daily averaged SWE-elevation chart for 5 days after a strong spring snowfall (occurred on 11th March 2004)

For the autumn snowfall (Figure 10), at the lower elevations SWE exhibits little dependence on elevation. In fact, snowfall has more or less the same intensity at the elevations higher than the snow limit (ranging from 700 m to 1000 m a.s.l.), but at the lower elevations snow was not formerly present at the ground. On the contrary, at the higher elevations other snowfalls had already occurred earlier with different snow limits, and this results in a linear relation. Some days after the snowfall, an increase in temperature causes rainfall events at the lower elevations, where

melting occurs, whereas at the higher elevations other snowfall events still occur, and the curve becomes steeper. For the winter snowfall (Figure 11), the relation is almost linear for all the elevations, as many other snowfall events had formerly occurred, and there is no melting. Concerning the early spring snowfall (Figure 12), just after the snowfall the relation is linear but after some days differential melting occurs at the lower elevations, this causes a steepening of the curve and an increase in its concavity, whereas at the higher elevations there is still snow accumulation.

In conclusion, the relation between SWE and elevation is more or less linear, but in autumn SWE is weekly dependent on elevation, whereas the dependence is very strong in spring, due to differential melting and to the succession of the snowfall events.

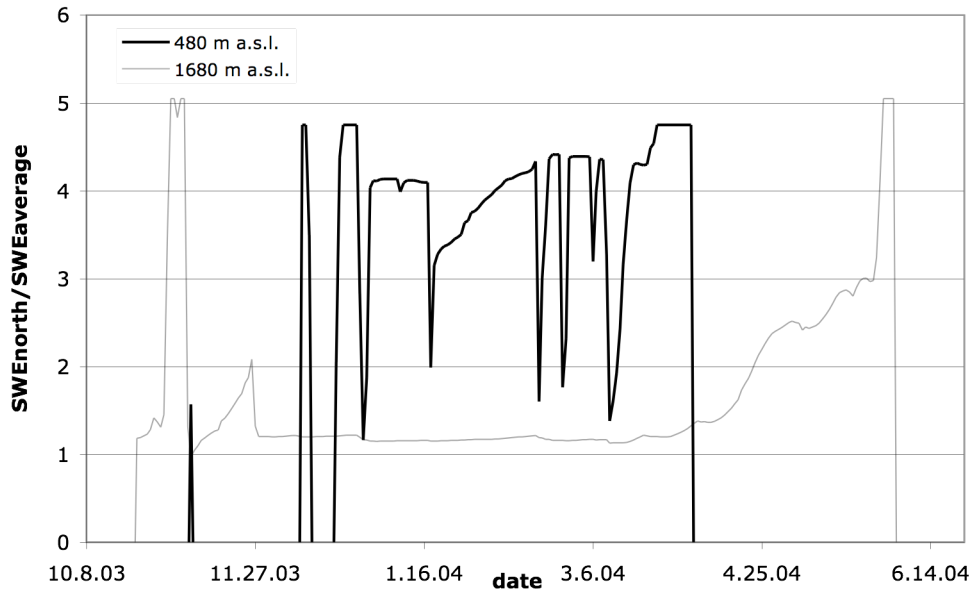


Figure 13: Time evolution of the ratio between SWE averaged only in north facing pixels and SWE averaged, for 2 elevation ranks

In Figure 13 the dependence of SWE on aspect is explored. The ratio between the SWE averaged in the north facing pixels and the SWE averaged in all pixels for each of the elevation ranks can be an index to evaluate the importance of the effects exerted by radiation and aspect. We consider as north facing pixels those characterized by aspect ranging from -20° to $+20^\circ$, being 0° the north aspect. Figure 13 shows the time evolution of this ratio for 2 different elevation ranks, one characteristic of the bottom of the valley and the other of the higher elevations. When the ratio is close to 1 no significant relation of SWE with aspect is present. When differential melting between N and S facing slopes occurs, the ratio increases to very high values. It can be noticed that in the bottom of the valley differential melting is always present all through the winter, except immediately after snowfalls. At the higher elevations, on the contrary, melting is aspect dominated only in autumn and in spring.

CONCLUSION

The comparison of the GEOtop SWE results with MODIS snow extent maps shows a fairly good agreement. The problems of the model are mainly due to uncertainties about the distribution of the meteorological forcing in space and time, as only measurements in some points are available. Only total precipitation is measured, and a criterion based on two thresholds on the air temperature has been used to distinguish solid and liquid precipitation. However, threshold values a little higher than the values found in literature were needed to reproduce the snow cover at the bottom of the valley. An hourly varying lapse rate was inferred by the temperature measurements, and was used as input data for the model.

Though characterized by some commission errors, MODIS maps can be valuable tools to validate distributed models. However, images of finer resolution and more frequent overpassing time would be better tools.

With the results of the model we investigated the relationship between SWE and elevation and aspect in different seasons. It has been shown that the dependence of SWE on elevation is more or less linear, but tends to be weaker in autumn and stronger in spring. Moreover, differential melting in north and south facing slopes occurs all through the winter at lower elevation (approximately below 800 m a.s.l.), whereas it is present only in autumn and in spring at the higher elevations. However, these relations should be verified in other applications to different and wider basins.

ACKNOWLEDGEMENT

We thank prof. John Albertson who supported the visit of the first author at the Department of Civil and Environmental Engineering of Duke University, and Joseph Tomasi who corrected a first version of the manuscript.

REFERENCES

- Alfnes E, Andreassen LM, Engeset RV, Skaugen T, Udnaes HC. 2004. Temporal variability in snow distribution. *Annals of Glaciology* **38**: 101-105.
- Anderson EA. 1976. *A point energy and mass balance model of a snow cover*. Office of Hydrology National Weather Service.
- Bertoldi G, Rigon R, Over TM. 2006. Impact of Watershed Geomorphic Characteristics on the Energy and Water Budgets. *Accepted to Journal of Hydrometeorology*.
- Brutsaert W. 2004. On a derivable formula for long-wave radiation from clear sky. *Water Resources Research* **11**: 742-744.
- Businger JA, Wyngaard JC, Izumi Y, Bradley EF. 2004. Flux-profile relationship in the atmospheric surface layer. *Journal of Atmospheric Sciences* **28**: 181-189.
- Carroll T, Cline D, Olheiser C, Rost A, Nilsson A, Fall G, Bovitz C, Li L. 2006. NOAA's national snow analyses. *Paper presented at the 74th Annual Meeting of the Western Snow Conference 2006*.
- Cazorzi F, Dalla Fontana G. 1996. Snowmelt modeling by combining air temperature and a distributed radiation index. *Journal of Hydrology* **181**: 169-187.
- Cline DW, Bales CB, Dozier J. Estimating the spatial distribution of snow in mountain basins using remote sensing and energy balance modeling. *Water Resources Research* **34**(5): 1275-1285.
- Cline D, Elder K, Bales R. 1998. Scale effects in a distributed snow water equivalence and snow melt model for mountain basins. *Hydrological Processes* **12**: 1527-1536.

- Colbeck SC, Anderson EA. 1982. The permeability of a melting snow cover. *Water Resources Research* **18**(4): 904-908.
- Hall DK, Andrew BT, James LF, Alfred TCC, Milan A. 2000. Intercomparison of satellite-derived snow-cover maps. *Annals of Glaciology* **31**: 369-376.
- Hall KH, Riggs GA, Salomonson VV, DiGirolamo NE, Bayr KJ. 2002. MODIS snow-cover products. *Remote Sensing of Environment* **83**: 181-194.
- Idso SB. 1981. A set of equation for full spectrum and 8 to 14 μm and 10.5 to 12.5 μm thermal radiation from cloudless skies. *Water Resources Research* **17**(2): 295-304.
- Iqbal M. 1983. *An introduction to solar radiation*. Academic Press.
- Jordan R. 1991. *A one dimensional temperature model for a snowcover: Technical documentation for SNTHERM 89, Spec. Rep. 657, User's guide*. US Army Cold Regions Research and Engineering Laboratory, Hanover, NH, USA.
- Lee S., Klein AG, Over TM. 2005. A comparison of MODIS and NOHRSC snow-cover products for simulating streamflow using the Snowmelt Runoff Model. *Hydrological Processes* **19**: 2951-2972.
- Marks D, Domingo J, Susong D, Link T, Garen D. 1999. A spatially distributed energy balance snowmelt model for application in mountain basins. *Hydrological Processes* **13**: 1935-1959.
- Martinec J, Rango A. 1986. Parameter values for snowmelt runoff modeling. *Journal of Hydrology* **84**: 197-219.
- Neteler M. 2005. Time series processing of MODIS satellite data for landscape epidemiological applications. *International Journal of Geoinformatics* **1**(1): 133-138.
- Oleson KW, Dai Y, Bonan G, Bosilovich M, Dickinson R, Dirmeyer P, Hoffman F, Houser P, Levis S, Niu G, Thornton P, Vertenstein M, Yang Z, Zeng X. 2004. *Technical description of the Community Land Model (CLM)*. NCAR, Boulder, CO, USA.
- Pomeroy JW, Toth B, Granger RJ, Hedstrom NR, Essery RLH. 2003. Variation in Surface Energetics during Snowmelt in a Subarctic Mountain Catchment. *Journal of Hydrometeorology* **4**: 702-719.
- Riggs GA, Hall DH, Salomonson VV. 2003. *MODIS Snow Products User Guide*. Electronic document: <http://modis-snow-ice.gsfc.nasa.gov/sugkc.html>.
- Riggs GA, Hall DK. 2006. Evaluation of snow errors in the MODIS snow data products. *Poster presented at the 63rd Annual Meeting of the Eastern Snow Conference 2006*.
- Rigon R, Bertoldi G, Over TM. 2006. GEOTop: A Distributed Hydrological Model with Coupled Water and Energy Budgets. *Accepted to Journal of Hydrometeorology*.
- Satterlund DR. 1979. An improved equation for estimating longwave radiation from the atmosphere. *Water Resources Research* **15**(6): 1649-1650.
- Turpin O, Ferguson R, Johansson B. 1999. Use of remote sensing to test and update simulated snow cover in hydrological models. *Hydrological Processes* **13**: 2067-2077.
- US Army Corps of Engineers. 1956. *Snow hydrology, Summary report of the snow investigations*. US Army Corps of Engineers, North Pacific Division, Portland, OR, USA.
- Zanotti F, Endrizzi S, Bertoldi G, Rigon R. 2004. The GEOTOP snow module. *Hydrological Processes* **18**: 3667-3679.